A homogeneous limit methodology and refinements of computationally efficient zigzag theory for homogeneous, laminated composite, and sandwich plates

A Homogeneous Limit Methodology and Refinements of Computationally Efficient Zigzag Theory for Homogeneous, Laminated Composite, and Sandwich Plates

Alexander Tessler,[1] **Marco Di Sciuva,**[2] **Marco Gherlone**[2]

[1] *Structural Mechanics and Concepts Branch, NASA Langley Research Center, M/S 190, Hampton, Virginia, 23681-2199*

[2] *Department of Aeronautics and Space Engineering, Politecnico di Torino, Corso Duca degli Abruzzi, 24, 10129, Torino, Italy*

The Refined Zigzag Theory (RZT) for homogeneous, laminated composite, and sandwich plates is revisited to offer a fresh insight into its fundamental assumptions and practical possibilities. The theory is introduced from a multiscale formalism starting with the inplane displacement field expressed as a superposition of coarse and fine contributions. The coarse displacement field is that of first-order shear-deformation theory, whereas the fine displacement field has a piecewise-linear zigzag distribution through the thickness. The resulting kinematic field provides a more realistic representation of the deformation states of transverse-shear-flexible plates than other similar theories. The condition of limiting homogeneity of transverse-shear properties is proposed and yields four distinct variants of zigzag functions. Analytic solutions for highly heterogeneous sandwich plates undergoing elastostatic deformations are used to identify the best-performing zigzag functions. Unlike previously used methods, which often result in anomalous conditions and nonphysical solutions, the present theory does not rely on transverse-shear-stress equilibrium constraints. For all material systems, there are no requirements for use of transverse-shear correction factors to yield accurate results. To model homogeneous plates with the full power of zigzag kinematics, infinitesimally small perturbations in the transverse shear properties are derived, thus enabling highly accurate predictions of homogeneous-plate behavior without the use of shear correction factors. The RZT predictive capabilities to model highly heterogeneous sandwich plates are critically assessed, demonstrating its superior efficiency, accuracy, and a wide range of applicability. This theory, which is derived from the virtual work principle, is well-suited for developing computationally efficient, C^0 a continuous function of (x_1, x_2) coordinates whose first-order derivatives are discontinuous along finite element interfaces and is thus appropriate for the analysis and design of high-performance load-bearing aerospace structures.
Numer Methods Partial Differential Eq 27: 208–229, 2011

Keywords: composite plates; plate theory; sandwich plates; shear deformation; virtual work principle; zigzag kinematics

Correspondence to: Marco Gherlone, Department of Aeronautics and Space Engineering, Politecnico di Torino, Corso Duca degli Abruzzi, 24, 10129, Torino, Italy (e-mail: marco.gherlone@polito.it)

I. INTRODUCTION

Advances in composites technology over the past four decades spurred an ever increasing use of composite materials in civilian and military aircraft, aerospace vehicles, naval, and civil structures. Application of composite materials leads to lightweight structures that offer high-performance and long-term durability and reliability. The newest state-of-the-art civilian aircraft, the Boeing 787, is 50% composite and uses carbon-epoxy materials for its fuselage, wings, and many load-bearing components.

Stress-analysis methods based on classical assumptions, which suppress the transverse shear and normal effects, have significant limitations particularly when applied to multilayered composites undergoing bending and transverse shear deformations. Load-bearing thick-section composites and sandwich structures can exhibit significant deformations due to transverse shear and thickness-stretch effects, especially in regions of stress concentration and when undergoing high-frequency responses. Many structural theories of first and higher order and their finite element implementations have been developed. The most widely used finite elements for plate and shell bending are those based on First-order Shear Deformation Theory (FSDT) [1–4], because of their computational efficiency and relatively wide range of applicability. Nevertheless, it is well recognized that such models have the tendency to underestimate the inplane strains and stresses, particularly in highly heterogeneous and thick composite and sandwich laminates, and overestimate natural frequencies of relatively high-frequency vibration modes [5–8]. Moreover, FSDT's accuracy is related to the use of shear correction factors that are material lay-up dependent. Higher-order theories, which take into account transverse shear deformability [8], are more accurate than FSDT and normally do not require shear correction factors. Theories based on the equivalent-single-layer assumption [9–12] also offer reduced computational complexity; however, they fail to model the zigzag-shaped cross-sectional distortion typical of heterogeneous laminates. Layer-wise theories [13, 14] have quasi-three-dimensional predictive capabilities; however, the computational effort is excessively great for most practical applications. To model sandwich laminates with sufficient accuracy commonly requires application of special sandwich theories to account for a zigzag-shaped, through-the-thickness distribution of inplane displacements and strains, at the expense of a much higher modeling and kinematic complexity [15–17]. Alternatively, three-dimensional finite element models are used to analyze relatively small structural regions of interest, and these are often coupled with two-dimensional discretizations to achieve smaller and computationally feasible models. Computational methods for nonlinear progressive failure analysis commonly employ cohesive elements and ply-by-ply discretizations, resulting in exceedingly intensive computations, particularly when large structures are analyzed [18, 19].

Zigzag theories pioneered by Di Sciuva, both in linear [20–23] and in cubic versions [24, 25], may be considered as a good compromise between adequate accuracy and low computational cost. The key idea is to add a piecewise-linear, zigzag-shaped (that is, C_z^0 a continuous function of z coordinate whose first-order derivative is discontinuous along material-layer interfaces) contribution to a globally linear or cubic through-the-thickness distribution of the inplane displacements. The superposed zigzag kinematics are determined in such a way as to satisfy equilibrium of the transverse shear stresses through the laminate thickness, as required by the theory of elasticity. The formulation results in a fixed number of kinematic unknowns, equal to that of FSDT, which does not depend on the number of layers. These theories often yield response predictions comparable to those of layer-wise theories; however, various flaws inherent in these theories have prevented their acceptance in practical applications.

Averill [26] recognized two major drawbacks that plague many previously mentioned zigzag theories: (i) C^1-continuous functions are required to approximate the deflection variable within

the finite element framework—the type of approximations that are especially undesirable for plate and shell finite elements and (ii) transverse shear stresses calculated from constitutive equations vanish erroneously along clamped boundaries.

Building on the observations of Averill [26], Tessler et al. presented [27–31] a Refined Zigzag Theory (RZT) that augments FSDT with a novel zigzag representation of the inplane displacements. The kinematic field does not require enforcement of transverse-shear-stress continuity to yield accurate results. Both drawbacks of the original zigzag theories are overcome because: (i) only first derivatives of the kinematic unknowns are present in the definition of the strain field, thus leading to C^0 -continuous shape functions for beam and plate finite elements [32–35] and (ii) all field equations (that is, equilibrium equations, constitutive equations, boundary conditions, and strain-displacement relations) are consistently derived from the virtual work principle without engendering any transverse-shear-force anomalies. Since the transverse shear forces are fully consistent with respect to the physical and variational requirements, they do not vanish erroneously along clamped boundaries. Furthermore, the theory has been demonstrated to yield consistently superior results over a wide range of aspect ratios and material systems, including thick laminates with a high degree of transverse shear flexibility, anisotropy, and heterogeneity.

In this article, the RZT [30] is revisited to reexamine its fundamental assumptions and to explore new modeling possibilities. In Section II, the theory is introduced from a multiscale formalism. The kinematic field is represented as a superposition of coarse and fine kinematic descriptions, where the coarse kinematics are those of FSDT and the fine kinematics are represented by piecewise C_z^0-continuous zigzag functions through the thickness. The definition of the zigzag functions is further refined by assuming that the coarse kinematics form the average laminate response only, whereas the fine kinematics represent a perturbation from the average response. The strain-displacement equations and constitutive relations are presented in Section III. In Section IV, the zigzag functions are defined in terms of layer-level thickness coordinates. The methodology for determining the zigzag functions from the transverse-shear constitutive relations is reviewed following the approach in [30]. Then, a new perspective, based on the concept of limiting homogeneity, is proposed for the determination of zigzag functions. This new methodology permits four distinct sets of zigzag functions to be obtained, one of which is coincident with the form derived in [30]. The concept of limiting homogeneity is further invoked for the purpose of modeling homogeneous plates with the full power of zigzag kinematics. Analytic results for homogeneous orthotropic plates and highly heterogeneous sandwich laminates are presented in Section V to demonstrate RZT's wide range of applicability.

II. KINEMATICS DESCRIPTION

Consider a multilayered composite plate of uniform thickness $2h$ composed of perfectly bonded orthotropic layers (or laminae) as shown in Fig. 1(a). Points of the plate are located by the orthogonal Cartesian coordinates (x_1, x_2, z) where x_1, x_2 are the reference coordinates with axes positioned in the middle plane of plate and z is the thickness coordinate axis. The ordered pair $(x_1, x_2) \in S_m$ denotes the inplane coordinates, where S_m represents the set of points given by the intersection of the plate with the plane $z = 0$, referred to herein as the middle reference plane (or midplane). The symbol $z \in [-h, h]$ denotes the domain of the through-the-thickness coordinate, with $z = 0$ identifying the plate's midplane. The plate is subjected to a normal-pressure loading, $q(x_1, x_2)$ applied at the midplane, S_m, which is defined as positive when acting in the positive z direction. In addition, a traction vector, $(\bar{T}_1, \bar{T}_2, \bar{T}_3)$, is prescribed on $S_\sigma \subset S$, where S denotes the total cylindrical-edge surface. On the remaining part of the edge surface, $S_u \subset S$, displacement restraints are imposed (or prescribed). The sections of the plate edge are related by $S_\sigma \cup S_u = S$

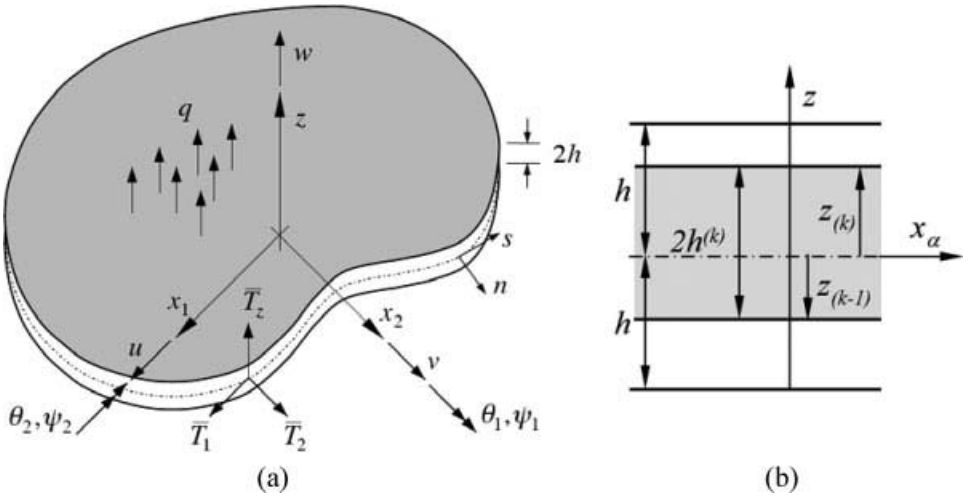

FIG. 1. (a) General plate notation and (b) lamination notation.

and $S_\sigma \cap S_u = \emptyset$. Moreover, the curves $C_\sigma = S_\sigma \cap S_m$ and $C_u = S_u \cap S_m$ define the two parts of the total perimeter $C = C_\sigma \cup C_u$ surrounding the midplane region, S_m. Finally, it is presumed that small-strain assumptions are valid, and that body and inertial forces are negligible.

The deformation of a plate subjected to applied loading and boundary restraints can be described by the displacement vector in terms of its Cartesian components as $\mathbf{u} \equiv (u_1^{(k)}, u_2^{(k)}, u_z^{(k)})$. Using a multiscale formalism, the material point at (x_1, x_2, z) situated within the kth material layer — which could be a ply or a fraction of a ply thickness, if the ply is further discretized through the thickness — is undergoing the displacement that may be expressed as a superposition of a coarse kinematic description $u_{i(c)}$ and a fine kinematic description $u_{i(f)}^{(k)}$ $(i = 1, 2, z)$, that is,

$$\begin{aligned} u_\alpha^{(k)}(x_1, x_2, z) &= u_{\alpha(c)}(x_1, x_2, z) + u_{\alpha(f)}^{(k)}(x_1, x_2, z) \quad (\alpha = 1, 2) \\ u_z^{(k)}(x_1, x_2, z) &= u_{z(c)}(x_1, x_2, z) + u_{z(f)}^{(k)}(x_1, x_2, z) \end{aligned} \tag{1}$$

where the superscript (k) $(k = 1, \ldots, N$, where N denotes the total number of material layers through the plate thickness) indicates that a quantity is dependent upon the kth layer constitutive properties; whereas, in the ensuing discussion, the subscript (k) defines quantities corresponding to the interface between the k and $(k + 1)$ layers. The kth layer thickness is defined in the range $[z_{(k-1)}, z_{(k)}]$ (see Fig. 1b).

To describe the coarse kinematics, first-order shear deformation theory (FSDT) can be used, in which case

$$\begin{aligned} u_{1(c)}(x_1, x_2, z) &\equiv u(x_1, x_2) + z\,\theta_1(x_1, x_2) \\ u_{2(c)}(x_1, x_2, z) &\equiv v(x_1, x_2) + z\,\theta_2(x_1, x_2) \\ u_z(x_1, x_2, z) &\equiv w(x_1, x_2) \end{aligned} \tag{2}$$

where u and v represent the constant through-the-thickness components of the in-plane displacements in the x_1 and x_2 coordinate directions, respectively; θ_1 and θ_2 represent average bending rotations of the transverse normal about the positive x_2 and the negative x_1 directions, respectively,

and they contribute to the linear distributions through the thickness; and w is the coarse or average description of transverse deflection.

For each displacement component in Eq. (1), the thickness-wise fine kinematic description with the resolution on the scale of the kth material layer is represented by linear functions defined in terms of the interface values of the kinematical variables, thus requiring $N + 1$ independent variables, where $N + 1$ is the total number of layer interfaces including the top and bottom plate surfaces. Therefore, in the definitions of $u^{(k)}_{\alpha(f)}$ and $u^{(k)}_{z(f)}$, $3 \times (N + 1)$ independent variables are required. This form of kinematics implies a layer-wise theory, having a high computational cost, comparable to that of three-dimensional elasticity theory, especially when applied to multilayered thick-section composite laminates for which N is large.

One way to reduce the number of unknowns in $u^{(k)}_{\alpha(f)}$ is first to represent these functions in terms of separable functions of the inplane (x_1, x_2) and transverse (z) coordinates, and then impose a set of interfacial constraint conditions, with this general strategy leading to what is commonly known as a zigzag formulation (e.g., see Di Sciuva [20]). A zigzag formulation reduces the number of kinematic unknowns to a small number that is independent of N, thus guaranteeing superior computational efficiency over layer-wise and three-dimensional elasticity methods. For many years it has been widely accepted that the interface constraint conditions to be used within a zigzag formulation should necessarily be conditions of perfect equilibrium of the transverse shear stresses along the layer interfaces. Whereas from the mechanics perspective the stress equilibrium needs to be perfectly satisfied, the limited kinematic freedom associated with the relatively simple displacements assumed a priori often lead to an over constraining of the kinematic field and subsequent pathological conditions and anomalies within the resulting theory.

In Tessler et al. [30], the fine displacement description is assumed as

$$\begin{aligned} u^{(k)}_{\alpha(f)}(x_1, x_2, z) &\equiv \phi^{(k)}_{\alpha}(z)\, \psi_{\alpha}(x_1, x_2) \\ u^{(k)}_{z(f)}(x_1, x_2, z) &\equiv 0 \end{aligned} \tag{3}$$

allowing only for the inplane displacements to have a fine description, where $\phi^{(k)}_{\alpha}(z)$ are piecewise-continuous through-the-thickness zigzag functions that stem from laminate heterogeneity, and $\psi_{\alpha}(x_1, x_2)$ are independent functions that may be interpreted as the amplitudes of the zigzag displacements. In its simplest form, as proposed by Tessler et al. [30], $\phi^{(k)}_{\alpha}(z)$ are piecewise linear, C^0-continuous functions through the thickness, having discontinuous thickness-derivatives $\phi^{(k)}_{\alpha,z}(z)$ at the layer interfaces.

The RZT of Tessler et al. [30] has seven kinematic variables (modes) regardless of the number of material layers through the thickness, with the kinematic field described by the orthogonal components of the displacement vector as

$$\begin{aligned} u^{(k)}_1(x_1, x_2, z) &\equiv u(x_1, x_2) + z\, \theta_1(x_1, x_2) + \phi^{(k)}_1(z)\, \psi_1(x_1, x_2) \\ u^{(k)}_2(x_1, x_2, z) &\equiv v(x_1, x_2) + z\, \theta_2(x_1, x_2) + \phi^{(k)}_2(z)\, \psi_2(x_1, x_2) \\ u_z(x_1, x_2, z) &\equiv w(x_1, x_2) \end{aligned} \tag{4}$$

During applied loading the material fiber, which prior to deformation is straight and perpendicular to the reference midplane, deforms and rotates about the x_α axes. The rotations, henceforth denoted as $\theta^{(k)}_{\alpha T}$, are given as

$$u^{(k)}_{\alpha,z} = \theta_{\alpha}(x_1, x_2) + \phi^{(k)}_{\alpha,z}(z)\, \psi_{\alpha}(x_1, x_2) \equiv \theta^{(k)}_{\alpha T} \tag{5}$$

where, henceforward, $(\bullet)_{,\alpha} \equiv \frac{\partial(\bullet)}{\partial x_\alpha}$ denotes a partial derivative with respect to the midplane coordinate, x_α. In Eq. (5), $\phi^{(k)}_{\alpha,z}$ are piecewise constant, and $\theta_\alpha(x_1, x_2)$ and $\psi_\alpha(x_1, x_2)$ are uniform with respect to the z coordinate; therefore, each material layer rotates in a piecewise constant manner described by the rotations $\theta^{(k)}_{\alpha T}$.

Integrating Eq. (5) over the laminate thickness and dividing by the total thickness gives the average rotations

$$\frac{1}{2h}\int_{-h}^{h} \theta^{(k)}_{\alpha T} dz = \theta_\alpha(x_1, x_2) + \left(\frac{1}{2h}\int_{-h}^{h} \phi^{(k)}_{\alpha,z}(z) dz\right) \psi_\alpha(x_1, x_2) \tag{6}$$

If the average rotations about the x_2 and x_1 axes of the initially normal fiber are represented by the coarse rotations $\theta_\alpha(x_1, x_2)$ only (as in Di Sciuva et al. [31]), then the following integral must vanish identically

$$\int_{-h}^{h} \phi^{(k)}_{\alpha,z}(z) dz = 0 \tag{7a}$$

Integration of Eq. (7a) results in the requirement that the top (surface) and bottom values of the respective zigzag functions are equal, that is,

$$\int_{-h}^{h} \phi^{(k)}_{\alpha,z}(z) dz = \phi^{(N)}_\alpha(h) - \phi^{(1)}_\alpha(-h) = 0 \tag{7b}$$

A special case of Eq. (7b) and a particularly convenient choice is to select the top and bottom values of the zigzag functions to vanish identically

$$\phi^{(1)}_\alpha(-h) = \phi^{(N)}_\alpha(h) = 0 \tag{8}$$

From Eqs. (4) and (8), the surface displacements are defined exclusively in terms of the coarse variables, that is,

$$\begin{array}{rcl} u^{(k)}_1(x_1, x_2, \pm h) & = & u(x_1, x_2) \pm h\, \theta_1(x_1, x_2) \\ u^{(k)}_2(x_1, x_2, \pm h) & = & v(x_1, x_2) \pm h\, \theta_2(x_1, x_2) \end{array} \tag{9}$$

III. STRAIN-DISPLACEMENT AND CONSTITUTIVE RELATIONS

The inplane and transverse shear strains derived from linear strain-displacement relations are

$$\varepsilon^{(k)}_{11} = u_{,1} + z\theta_{1,1} + \phi^{(k)}_1 \psi_{1,1}, \tag{10a}$$

$$\varepsilon^{(k)}_{22} = v_{,2} + z\theta_{2,2} + \phi^{(k)}_2 \psi_{2,2}, \tag{10b}$$

$$\gamma^{(k)}_{12} = u_{,2} + v_{,1} + z(\theta_{1,2} + \theta_{2,1}) + \phi^{(k)}_1 \psi_{1,2} + \phi^{(k)}_2 \psi_{2,1}, \tag{10c}$$

$$\gamma^{(k)}_{\alpha z} = w_{,\alpha} + \theta_\alpha + \phi^{(k)}_{\alpha,z}\, \psi_\alpha \quad (\alpha = 1, 2). \tag{10d}$$

The zigzag-function property given by Eq. (7a) ensures that the average transverse shear strains (γ_α) are those which correspond to FSDT (a coarse description), that is,

$$\gamma_\alpha = \frac{1}{2h}\int_{-h}^{h} \gamma^{(k)}_{\alpha z} dz = w_{,\alpha} + \theta_\alpha. \tag{11}$$

The generalized Hooke's law for the kth orthotropic material layer, whose principal material directions are arbitrary with respect to the reference coordinates $(x_1, x_2) \in S_m$, is expressed as

$$\begin{Bmatrix} \sigma_{11} \\ \sigma_{22} \\ \tau_{12} \\ \tau_{2z} \\ \tau_{1z} \end{Bmatrix}^{(k)} = \begin{bmatrix} C_{11} & C_{12} & C_{16} & 0 & 0 \\ C_{12} & C_{22} & C_{26} & 0 & 0 \\ C_{16} & C_{26} & C_{66} & 0 & 0 \\ 0 & 0 & 0 & Q_{22} & Q_{12} \\ 0 & 0 & 0 & Q_{12} & Q_{11} \end{bmatrix}^{(k)} \begin{Bmatrix} \varepsilon_{11} \\ \varepsilon_{22} \\ \gamma_{12} \\ \gamma_{2z} \\ \gamma_{1z} \end{Bmatrix}^{(k)}, \tag{12a}$$

where $C_{ij}^{(k)}$ and $Q_{ij}^{(k)}$ are the transformed elastic-stiffness coefficients referred to the (x_1, x_2, z) coordinate system, relative to the stress condition that ignores the transverse-normal stress. To aid in subsequent discussions, expressions for $Q_{ij}^{(k)}$ are given in terms of their principal transverse-shear moduli, $G_{13}^{(k)}$ and $G_{23}^{(k)}$, and an angle $\theta^{(k)}$ (the angle between the principal material direction x_1' and the x_1 axis, formed by the right-hand rule)

$$\begin{aligned} &Q_{11}^{(k)} = \cos^2(\theta^{(k)})\, G_{13}^{(k)} + \sin^2(\theta^{(k)})\, G_{23}^{(k)};\ Q_{12}^{(k)} = \sin(\theta^{(k)})\, \cos(\theta^{(k)})\, \left(G_{13}^{(k)} - G_{23}^{(k)}\right); \\ &Q_{22}^{(k)} = \cos^2(\theta^{(k)})\, G_{23}^{(k)} + \sin^2(\theta^{(k)})\, G_{13}^{(k)}. \end{aligned} \tag{12b}$$

IV. ZIGZAG FUNCTIONS AND TRANSVERSE SHEAR CONSTITUTIVE RELATIONS

The refined zigzag functions (or zigzag displacements) of the present theory are defined by piecewise linear, C_z^0-continuous functions (that is, C^0-continuous functions through the laminate thickness.) For convenience, the zigzag functions $\phi_\alpha^{(k)}(z)$ $(\alpha = 1, 2)$, which have units of length, are defined in terms of their respective layer-interface values $\phi_{\alpha(i)}$ $(i = 0, 1, \ldots, N)$ (see Fig. 2 depicting the notation for a three-layered laminate). For the kth material layer located in the range $[z_{(k-1)},\ z_{(k)}]$, the zigzag functions are given as

$$\phi_\alpha^{(k)} \equiv \frac{1}{2}(1 - \zeta^{(k)})\phi_{\alpha(k-1)} + \frac{1}{2}(1 + \zeta^{(k)})\phi_{\alpha(k)}, \tag{13}$$

$$\zeta^{(k)} = [(z - z_{(k-1)})/h^{(k)} - 1] \in [-1, 1] \quad (k = 1, \ldots, N) \tag{14}$$

with the first layer beginning at $z_{(0)} = -h$, the last Nth layer ending at $z_{(N)} = h$, and the kth layer ending at $z_{(k)} = z_{(k-1)} + 2h^{(k)}$, where $2h^{(k)}$ denotes the kth layer thickness and $\zeta^{(k)}$ is the dimensionless thickness coordinates of the kth material layer.

Evaluating Eq. (13) at the layer interfaces gives rise to the definitions of the interface displacements

$$\phi_{\alpha(k-1)} = \phi_\alpha^{(k)}(\zeta^{(k)} = -1), \quad \phi_{\alpha(k)} = \phi_\alpha^{(k)}(\zeta^{(k)} = 1), \tag{15}$$

where, according to Eq. (8), the top and bottom interfacial displacements are set to vanish

$$\phi_{\alpha(0)} = \phi_{\alpha(N)} = 0. \tag{16}$$

Differentiating Eq. (13) with respect to the z coordinate yields the piecewise-constant functions

$$\phi_{\alpha,z}^{(k)} = \frac{1}{2h^{(k)}}(\phi_{\alpha(k)} - \phi_{\alpha(k-1)}). \tag{17}$$

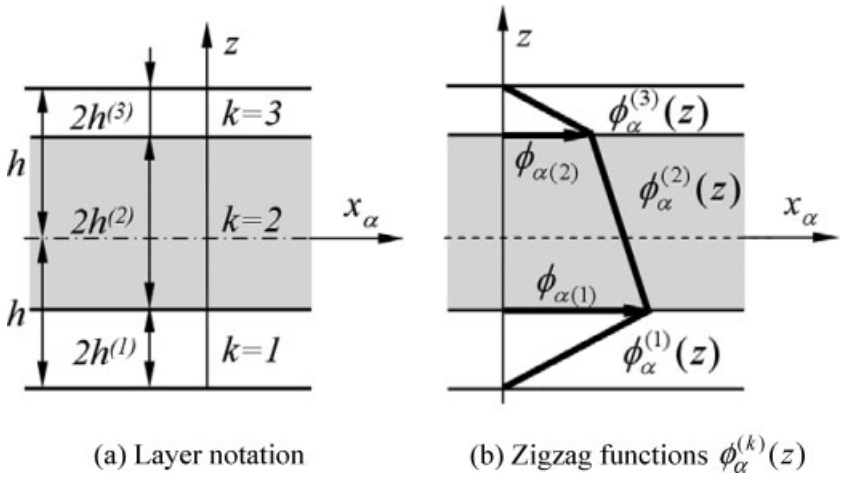

FIG. 2. Notation for a three-layered laminate and $\phi_\alpha^{(k)}(z)$ zigzag functions defined in terms of interface displacements $\phi_{\alpha(k)}$.

Straightforward algebraic manipulations provide the alternative forms for $\phi_\alpha^{(k)}(z)$ in terms of $\phi_{\alpha,z}^{(k)}(z)$

$$\phi_\alpha^{(k)} = \phi_{\alpha,z}^{(k)}(z - z_{(k-1)}) + \phi_{\alpha(k-1)} \tag{18}$$

A. Preceding Methodology for Zigzag Function Selection

The approach in zigzag function selection according to Tessler et al. [30] begins by expressing the transverse shear stresses in the following form

$$\begin{Bmatrix} \tau_{1z} \\ \tau_{2z} \end{Bmatrix}^{(k)} \equiv \begin{bmatrix} Q_{11} & Q_{12} \\ Q_{12} & Q_{22} \end{bmatrix}^{(k)} \left(\begin{Bmatrix} \gamma_1 - \psi_1 \\ \gamma_2 - \psi_2 \end{Bmatrix} + \begin{Bmatrix} 1 + \phi_{1,z}^{(k)} \\ 0 \end{Bmatrix} \psi_1 + \begin{Bmatrix} 0 \\ 1 + \phi_{2,z}^{(k)} \end{Bmatrix} \psi_2 \right) \tag{19a}$$

or alternatively as

$$\begin{aligned} \begin{Bmatrix} \tau_{1z} \\ \tau_{2z} \end{Bmatrix}^{(k)} \equiv & \begin{bmatrix} Q_{11} & Q_{12} \\ Q_{12} & Q_{22} \end{bmatrix}^{(k)} \begin{Bmatrix} \gamma_1 - \psi_1 \\ \gamma_2 - \psi_2 \end{Bmatrix} \\ & + Q_{11}^{(k)} \left(1 + \phi_{1,z}^{(k)}\right) \begin{Bmatrix} 1 \\ Q_{12}^{(k)}/Q_{11}^{(k)} \end{Bmatrix} \psi_1 + Q_{22}^{(k)} \left(1 + \phi_{2,z}^{(k)}\right) \begin{Bmatrix} Q_{12}^{(k)}/Q_{22}^{(k)} \\ 1 \end{Bmatrix} \psi_2 \end{aligned} \tag{19b}$$

In Eq. (19b), the second and third stress vectors include, as their normalization (or scaling) factors, coefficients $Q_{\alpha\alpha}^{(k)}(1 + \phi_{\alpha,z}^{(k)})$ ($\alpha = 1, 2$) involving their respective zigzag functions. If the normalization factors are selected to be constant for all material layers, that is,

$$Q_{\alpha\alpha}^{(k)}\left(1 + \phi_{\alpha,z}^{(k)}\right) \equiv G_\alpha \tag{20}$$

where G_α are yet undetermined constants, then solving Eq. (20) for $\phi_{\alpha,z}^{(k)}$ results in

$$\phi_{\alpha,z}^{(k)} = G_\alpha / Q_{\alpha\alpha}^{(k)} - 1 \tag{21}$$

Substituting Eq. (21) into Eq. (7a) reveals that the G_α constants represent some weighted-average transverse-shear stiffness coefficients of a laminate given by

$$G_\alpha = \left(\frac{1}{2h} \int_{-h}^{h} \frac{dz}{Q_{\alpha\alpha}^{(k)}} \right)^{-1} = \left(\frac{1}{h} \sum_{k=1}^{N} \frac{h^{(k)}}{Q_{\alpha\alpha}^{(k)}} \right)^{-1} \tag{22}$$

Using Eq. (17), all interfacial displacements ($\phi_{\alpha(k)}$) are readily determined in terms of $\phi_{\alpha,z}^{(k)}$ as

$$\phi_{\alpha(k)} = \phi_{\alpha(k-1)} + 2h^{(k)} \phi_{\alpha,z}^{(k)} \tag{23a}$$

Accounting for the homogeneous boundary conditions, Eq. (16), the interfacial displacements are further simplified as

$$\phi_{\alpha(k)} = \sum_{i=1}^{k} 2h^{(i)} \phi_{\alpha,z}^{(i)} \tag{23b}$$

With $\phi_{\alpha,z}^{(k)}$ and G_α fully defined by Eqs. (21) and (22), the definitions of the zigzag functions given by Eq. (18) are complete. Invoking Eqs. (10d) and (22), piecewise-constant distributions of the transverse shear strains are maintained and are given as

$$\gamma_{\alpha z}^{(k)} = w_{,\alpha} + \theta_\alpha + \left[\left(\frac{Q_{\alpha\alpha}^{(k)}}{h} \sum_{k=1}^{N} \frac{h^{(k)}}{Q_{\alpha\alpha}^{(k)}} \right)^{-1} - 1 \right] \psi_\alpha \tag{24}$$

Note that the present methodology for deriving the zigzag functions is purely constitutive-based; in contrast to the previous zigzag models, there exist no kinematic constraints. In [30], extensive analytical studies for simply supported and clamped laminated composite and sandwich plates have been carried out and have demonstrated superior modeling capabilities of this theory.

B. Homogeneous Limit Methodology for Zigzag Function Selection

In what follows a new methodology for obtaining suitable zigzag functions is examined. The approach exploits an intrinsic property of zigzag functions referred to herein as the homogeneous limit property. It is postulated that a zigzag function $\phi_\alpha^{(k)}$ ($\alpha = 1, 2; k = 1, \ldots, N$) has a non-vanishing distribution provided that the layer-wise transverse shear properties on the x_α cross-sections are different, that is, when the material layers are heterogeneous with respect to their transverse shear properties. The converse of this property is that under the homogeneous limit defined as

$$Q_{\alpha\alpha}^{(k)} \to G_\alpha \tag{25}$$

where G_α are the constant transverse-shear moduli corresponding to the x_α planes (that is, the planes normal to the x_α coordinate axes), the zigzag functions are required to vanish in a limiting sense under all admissible deformations, that is,

$$\phi_\alpha^{(k)}(z) \to 0 \quad if \quad Q_{\alpha\alpha}^{(k)} \to G_\alpha \tag{26}$$

The homogeneous-limit conditions, Eq. (25), also imply that all material layers have the same angular orientation, $\theta^{(k)}$. It immediately follows from Eq. (26) that $\phi_{\alpha,z}^{(k)}$ also vanish in a limiting sense [refer to Eq. (18)], that is,

$$\phi_{\alpha,z}^{(k)} \to 0 \quad if \quad Q_{\alpha\alpha}^{(k)} \to G_\alpha \tag{27}$$

Moreover, the limiting conditions described by Eqs. (26) and (27) guarantee that all interior interfacial displacements of the zigzag functions must vanish in a limiting sense as the laminate approaches its homogeneous limit

$$\phi_{\alpha(i)} \to 0 \quad (i = 1, \ldots, N-1) \tag{28}$$

whereas the exterior (bottom and top) interfacial displacements have been set to zero explicitly in Eq. (16). Rewriting Eq. (25) by moving G_α to the left-hand side of the equation, and then dividing by $Q_{\alpha\alpha}^{(k)}$ or by G_α, gives two sets of dimensionless functions labeled as $g_\alpha^{(k)}$ and $g_{I\alpha}^{(k)}$:

$$\left(g_\alpha^{(k)}, g_{I\alpha}^{(k)}\right) \equiv \left(G_\alpha / Q_{\alpha\alpha}^{(k)} - 1,\, Q_{\alpha\alpha}^{(k)} / G_{I\alpha} - 1\right) \tag{29}$$

where, for expediency, G_α has been renamed as $G_{I\alpha}$ in the definition of $g_{I\alpha}^{(k)}$. It can be seen that $g_\alpha^{(k)}$ and $g_{I\alpha}^{(k)}$ have the same characteristics as $\phi_{\alpha,z}^{(k)}$; specifically, (1) these functions are dimensionless, piecewise-constant, and dependent upon the kth layer's transverse shear stiffnesses, and (2) each of these functions vanishes in a limiting sense under the homogeneous limit, Eq. (25). Therefore, either $g_\alpha^{(k)}$ and $g_{I\alpha}^{(k)}$ can be considered to represent $\phi_{\alpha,z}^{(k)}$ and thus complete the definition of the zigzag functions.

Specifically:

G_α Method. Exploring the possibility of $g_\alpha^{(k)}$ to represent $\phi_{\alpha,z}^{(k)}$ and setting

$$\phi_{\alpha,z}^{(k)} \equiv g_\alpha^{(k)} = G_\alpha / Q_{\alpha\alpha}^{(k)} - 1 \tag{30}$$

it is observed that Eqs. (21) and (30) are identical. Moreover, by invoking Eq. (7a), the definition for G_α given by Eq. (22) is obtained.

$G_{I\alpha}$ Method. When $g_{I\alpha}^{(k)}$, given by the second relation in Eq. (29), is taken as a representation for $\phi_{\alpha,z}^{(k)}$, there results

$$\phi_{\alpha,z}^{(k)} \equiv g_{I\alpha}^{(k)} = Q_{\alpha\alpha}^{(k)} / G_{I\alpha} - 1. \tag{31}$$

Substituting this expression into Eq. (7a) yields yet another set of weighted-average constants

$$G_{I\alpha} = \frac{1}{h} \sum_{k=1}^{N} h^{(k)} Q_{\alpha\alpha}^{(k)}, \tag{32}$$

and, consequently, with the use of Eqs. (13) and (23b), another set of zigzag functions is obtained.

Note that G_α and $G_{I\alpha}$ represent two different weighted-average transverse shear properties of a laminate. In both cases, however, there exists dependence on the principal transverse shear moduli of each individual layer as well as their orientation angles $\theta^{(k)}$.

Alternatively, the *homogeneous limit strategy* can be applied by examining the transverse-shear compliance coefficients instead of the stiffness coefficients. Hooke's relations for the k-th material

layer in terms of the transformed compliance coefficients that relate the transverse shear strains to their conjugate stresses may be written as

$$\begin{Bmatrix} \gamma_{1z} \\ \gamma_{2z} \end{Bmatrix}^{(k)} = \begin{bmatrix} S_{11} & S_{12} \\ S_{12} & S_{22} \end{bmatrix}^{(k)} \begin{Bmatrix} \tau_{1z} \\ \tau_{2z} \end{Bmatrix}^{(k)} . \tag{33}$$

Therefore, the homogeneous limit conditions for $\phi_{\alpha,z}^{(k)}$ and the compliance coefficients corresponding to the x_α planes may be written

$$\phi_{\alpha,z}^{(k)} \to 0 \quad if \quad S_{\alpha\alpha}^{(k)} \to C_\alpha \tag{34}$$

where C_α are yet undetermined constants.

Following the procedure outlined in Eqs. (28)–(32), two additional functions can be considered to represent $\phi_{\alpha,z}^{(k)}$, that is,

$$\left(c_\alpha^{(k)}, c_{I\alpha}^{(k)}\right) \equiv \left(C_\alpha / S_{\alpha\alpha}^{(k)} - 1, S_{\alpha\alpha}^{(k)} / C_{I\alpha} - 1\right) \tag{35}$$

The two additional possible representations for the zigzag functions are

C_α Method. Herein $c_\alpha^{(k)}$ is set to represent $\phi_{\alpha,z}^{(k)}$, that is,

$$\phi_{\alpha,z}^{(k)} \equiv c_\alpha^{(k)} = C_\alpha / S_{\alpha\alpha}^{(k)} - 1 \tag{36}$$

Substituting Eq. (36) into Eq. (7a) yields

$$C_\alpha = \left(\frac{1}{h} \sum_{k=1}^{N} \frac{h^{(k)}}{S_{\alpha\alpha}^{(k)}} \right)^{-1} \tag{37}$$

$C_{I\alpha}$ Method. Letting $c_{I\alpha}^{(k)}$ to represent $\phi_{\alpha,z}^{(k)}$, there results

$$\phi_{\alpha,z}^{(k)} \equiv c_{I\alpha}^{(k)} = S_{\alpha\alpha}^{(k)} / C_{I\alpha} - 1 \tag{38}$$

Substituting Eq. (38) into Eq. (7a) yields

$$C_{I\alpha} = \frac{1}{h} \sum_{k=1}^{N} h^{(k)} S_{\alpha\alpha}^{(k)} \tag{39}$$

where it is noted that C_α and $C_{I\alpha}$ are two different weighted-average laminate constants for a given laminate. For the special case of a diagonal compliance/stiffness matrix representing all layers ($Q_{12}^{(k)} = 0$), such as in a cross-ply laminate whose principal material directions are aligned with the Cartesian plate coordinates, it can be readily verified that

$$(C_\alpha, C_{I\alpha}) = \left(G_{I\alpha}^{-1}, G_\alpha^{-1}\right) \quad \text{and} \quad \left(c_\alpha^{(k)}, c_{I\alpha}^{(k)}\right) = \left(g_{I\alpha}^{(k)}, g_\alpha^{(k)}\right) \tag{40}$$

The four zigzag-function methods are summarized in Table I. In Section V, these methods are examined quantitatively by way of analytic solutions for simply supported sandwich plates.

TABLE I. Zigzag function definitions.

Homogeneous limit method	Weighted-average constants	Zigzag-function derivatives $\phi_{\alpha,z}^{(k)}$	Interfacial displacements
1	$G_\alpha = \left(\frac{1}{h}\sum_{k=1}^{N}\frac{h^{(k)}}{Q_{\alpha\alpha}^{(k)}}\right)^{-1}$	$g_\alpha^{(k)} = G_\alpha/Q_{\alpha\alpha}^{(k)} - 1$	$\phi_{\alpha(k)} = \sum_{i=1}^{k} 2h^{(i)}\,\phi_{\alpha,z}^{(i)}$
2	$G_{I\alpha} = \frac{1}{h}\sum_{k=1}^{N} h^{(k)} Q_{\alpha\alpha}^{(k)}$	$g_{I\alpha}^{(k)} = Q_{\alpha\alpha}^{(k)}/G_{I\alpha} - 1$	
3	$C_\alpha = \left(\frac{1}{h}\sum_{k=1}^{N}\frac{h^{(k)}}{S_{\alpha\alpha}^{(k)}}\right)^{-1}$	$c_\alpha^{(k)} = C_\alpha/S_{\alpha\alpha}^{(k)} - 1$	
4	$C_{I\alpha} = \frac{1}{h}\sum_{k=1}^{N} h^{(k)} S_{\alpha\alpha}^{(k)}$	$c_{I\alpha}^{(k)} = S_{\alpha\alpha}^{(k)}/C_{I\alpha} - 1$	

C. Modeling Homogeneous Plates With the Full Power of Zigzag Kinematics

When modeling homogeneous plates or laminated plates with the same transverse shear stiffnesses on the planes of rectilinear orthotropy, the RZT can be successfully applied by invoking the homogeneous-limit property. To achieve accurate predictions for homogeneous plates without the use of shear correction factors, the differences in the layer transverse shear moduli can be made arbitrarily small, with such an approach taking the full advantage of zigzag kinematics. A judicious choice of small perturbations to describe nearly homogeneous transverse shear properties over the plate's thickness can lead to remarkably accurate predictions, achieving parabolic shear strain and stress distributions that are consistent with elasticity theory predictions for homogeneous plates. Moreover, the approach yields accurate nonlinear inplane strains and stresses when modeling thick plates. By contrast, the use of purely homogeneous transverse shear properties would result in the vanishing of the zigzag functions and would lead to the exclusively coarse theory, known as FSDT; where, for homogeneous plates, the kinematic assumptions give rise to constant through-the-thickness transverse shear strains and stresses and linear inplane strains and stresses, thus requiring a shear correction factor to compensate, in an average sense, for the lack of the parabolic transverse shear distributions.

The approach is demonstrated by using the RZT based on the G_α method (see Table I). For simplicity and clarity of the discussion, a laminated plate whose principal axes of rectilinear orthotropy are coincident with the x_1 and x_2 plate axes (thus $Q_{11}^{(k)} = G_{13}^{(k)}$, $Q_{22}^{(k)} = G_{23}^{(k)}$, $Q_{12}^{(k)} = 0$) is considered; further, cylindrical bending about the x_2 axis is considered so that the response quantities are functions of only the x_1 and z coordinates. Using Eqs. (10d) and (11), the RZT yields the following expression for the transverse shear strain

$$\gamma_{1z}^{(k)} = \gamma_1(x_1)\left[1 + \phi_{1,z}^{(k)}\frac{\psi_1(x_1)}{\gamma_1(x_1)}\right]. \tag{41}$$

It is then assumed that the material layers have slightly different shear moduli from a constant value G_{13}

$$G_{13}^{(k)} = G_{13}(1 + \varepsilon^{(k)}) \quad (k = 1, \ldots, N), \tag{42}$$

where $\varepsilon^{(k)} \equiv s\mu^{(k)} \ll 1$ with $\mu^{(k)} = O(1)$ denoting a dimensionless piecewise-constant function and s an arbitrarily small scalar. Substituting Eq. (42) into Eq. (22) and using Eq. (21) yields

$$G_1 \simeq G_{13} \quad \text{and} \quad \phi_{1,z}^{(k)} \simeq -s\mu^{(k)}. \tag{43}$$

Note that both $\psi_1(x_1)$ and $\gamma_1(x_1)$ have the same functional form in terms of x_1; also, for this nearly homogeneous case their magnitudes are respectively $O(s^{-1})$ and $O(1)$. Therefore, the ratio of the two functions appearing in Eq. (41) is simply a large constant

$$\frac{\psi_1(x_1)}{\gamma_1(x_1)} = O(s^{-1}). \tag{44}$$

Accounting for Eqs. (43) and (44) yields the transverse shear strain of the form

$$\gamma_{1z}^{(k)} = \gamma_1(x_1)(1 - c\mu^{(k)}), \tag{45}$$

where c is a dimensionless constant and $(1 - c\mu^{(k)})$ represents a piecewise constant thickness distribution of the transverse shear strain.

A parabolic transverse shear distribution is a good approximation for homogeneous plates that range from moderately thick to thin plates. Therefore, for the cylindrical bending problem considered herein a parabolic distribution of the transverse shear strain may be expressed as

$$\gamma_{1z}^{H} = \Gamma_1(x_1)\left(1 - \frac{z^2}{h^2}\right), \tag{46}$$

where the $\Gamma_1(x_1)$ function is determined from a given boundary value problem.

The function $\mu^{(k)}$ in Eq. (45) can now be determined in such a way as to allow $(1 - c\mu^{(k)})$ to approximate a parabolic distribution given by Eq. (46) in an average sense. Thus, the average shear strain across the kth layer resulting from Eq. (46) is set to correspond to $(1 - c\mu^{(k)})$, that is,

$$\frac{1}{2h^{(k)}}\int_{z_{(k-1)}}^{z_{(k)}}\left(1 - \frac{z^2}{h^2}\right)dz = 1 - \frac{z_{(k-1)}^2 + z_{(k)}^2 + z_{(k-1)}z_{(k)}}{3h^2} = 1 - c\mu^{(k)}, \tag{47}$$

from which

$$\mu^{(k)} = \frac{1}{3c}\left(\frac{z_{(k-1)}^2}{h^2} + \frac{z_{(k)}^2}{h^2} + \frac{z_{(k-1)}z_{(k)}}{h^2}\right), \tag{48}$$

and, finally,

$$\varepsilon^{(k)} = s\left(\frac{z_{(k-1)}^2}{h^2} + \frac{z_{(k)}^2}{h^2} + \frac{z_{(k-1)}z_{(k)}}{h^2}\right) \ll 1, \tag{49}$$

where the constant $3c$ has been absorbed into an arbitrarily small scalar $s \ll 1$.

A similar analysis of cylindrical bending about the x_1 axis results in the expressions for the $G_{23}^{(k)}$ transverse shear moduli

$$G_{23}^{(k)} = G_{23}(1 + \varepsilon^{(k)}), \tag{50}$$

where $\varepsilon^{(k)}$ is the same as that given in Eq. (49).

Equations (42), (49), and (50) provide the slightly perturbed transverse-shear-modulus distributions through the thickness, for the purpose of achieving a homogeneous plate in a limiting sense as the small parameter $\varepsilon^{(k)}$ diminishes to zero and the number of discretized layers N becomes sufficiently large.

D. Remarks on Equilibrium Equations, Boundary Conditions, and FEM Approximations

The plate equilibrium equations and consistent boundary conditions are derived in [30] from the virtual work principle, resulting in a system of seven second-order partial differential equilibrium equations in terms of the seven kinematic variables, thus constituting a 14th-order theory. The number of kinematic variables within this theory is fixed at seven and does not depend on the number of discretized layers; hence the computational effort is practically the same for any number N. From the computational perspective of finite element approximations, C^0-continuous kinematic functions can be used because the strain measures are represented by partial derivatives not exceeding first order.

V. EXAMPLE PROBLEMS AND RESULTS

Analytic solutions for simply supported square laminates are used to examine the predictive capability of the four variants of the present RZT. The plate is defined on the domain $x_1 \in [0, a]$, $x_2 \in [0, a]$, $z \in [-h, h]$ and is subjected to the sinusoidal transverse loading $q = q_0 \sin(\pi x_1/a) \sin(\pi x_2/a)$. The analytic solutions for uniaxial, cross-ply, and angle-ply laminates are derived in [30]. The first set of example problems examines the modeling of thin, moderately thick, and thick homogeneous orthotropic plates using the perturbed transverse-shear approach. Then, results for a highly heterogeneous and anisotropic angle-ply antisymmetric sandwich laminate are critically examined. The numerical and graphical results that follow include results of the four variants of RZT and several other theories that are used for comparison purposes; the results are labeled as:

3D Elasticity:	Three-dimensional elasticity solutions using procedures developed by Pagano [36] for cross-ply laminated plates and by Noor and Burton [37] for angle-ply antisymmetric laminates.
FSDT:	First-order Shear Deformation Theory; shear correction factor $k^2 = 5/6$.
Reddy:	Third-order equivalent single-layer theory by Reddy [9].
Zigzag (D):	Di Sciuva theory [23].
RZT (G_α):	Refined zigzag theory based on the G_α method (refer to Table I).
RZT (G_α; N):	Refined zigzag theory based on the G_α method modeling a homogeneous plate with N discretized layers through the thickness (refer to Figs. 3–5).
RZT ($G_{I\alpha}$):	Refined zigzag theory based on the $G_{I\alpha}$ method (refer to Table I).
RZT (C_α):	Refined zigzag theory based on the C_α method (refer to Table I).
RZT ($C_{I\alpha}$):	Refined zigzag theory based on the $C_{I\alpha}$ method (refer to Table I).

In Figs. 3–8, the through-the-thickness distributions correspond to the normalized displacement and stresses, given as

$$\bar{u}_1 = (10^4 D_{11}/q_o a^4) u_1^{(k)}(0, a/2, z), \bar{\sigma}_{11} \equiv ((2h)^2/q_0 a^2)\sigma_{11}^{(k)}(a/2, a/2, z), \text{ and}$$

$$\bar{\tau}_{1z} \equiv (2h/q_0 a)\tau_{1z}^{(k)}(0, a/2, z).$$

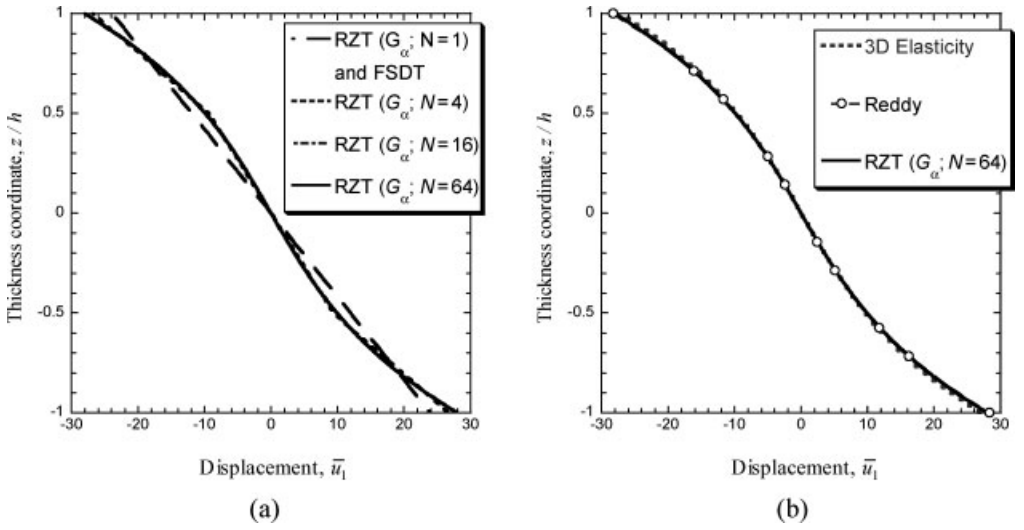

FIG. 3. Through-thickness distribution of inplane displacement for a homogeneous orthotropic plate (a/2h = 5).

A. Homogeneous Orthotropic Plates

The ability of RZT to model homogeneous orthotropic plates using the perturbed transverse-shear approach is demonstrated subsequently. The plate is made of a carbon-epoxy material with the mechanical properties given by Young's moduli $E_1^{(k)} = 1.579 \times 10^2$ GPa, $E_2^{(k)} = E_3^{(k)} = 9.584$ GPa, Poisson ratios $v_{12}^{(k)} = v_{13}^{(k)} = 0.32$, $v_{23}^{(k)} = 0.49$, and shear moduli $G_{12}^{(k)} = G_{13}^{(k)} = 5.930$ GPa, and $G_{23}^{(k)} = 3.227$ GPa. For this homogeneous, orthotropic plate the principal material directions are aligned with the plate coordinate axes.

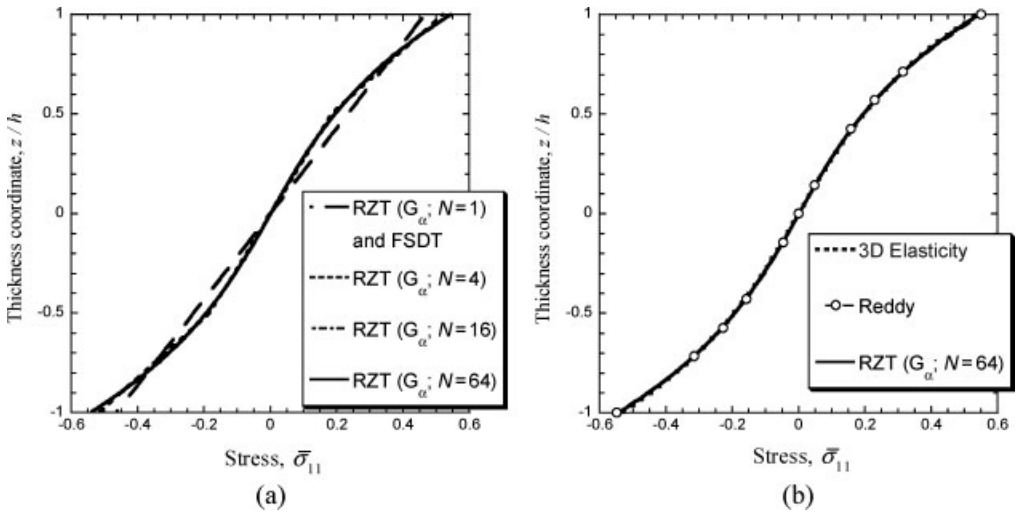

FIG. 4. Through-thickness distribution of inplane stress for a homogeneous orthotropic plate (a/2h = 5).

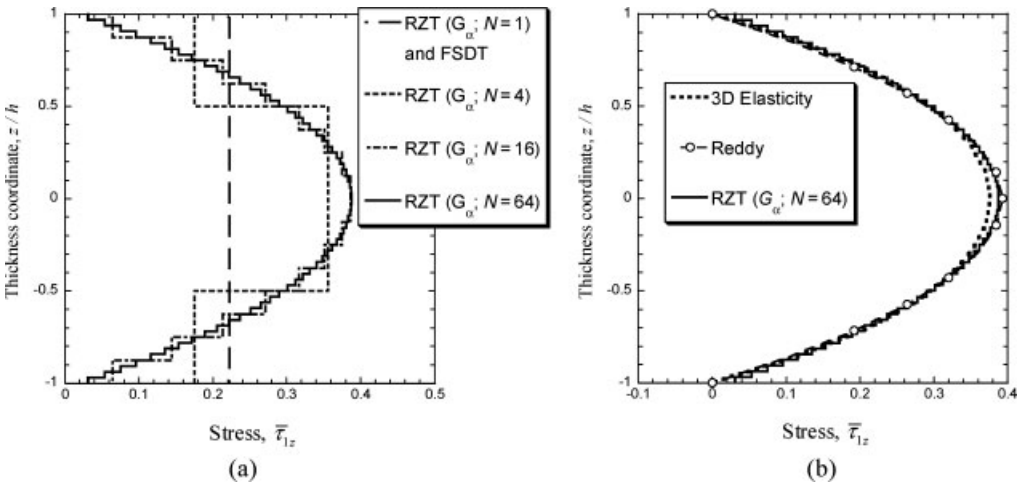

FIG. 5. Through-thickness distribution of transverse shear stress for a homogeneous orthotropic plate (a/2h = 5).

The four variants of RZT, when applied to the carbon-epoxy (homogeneous and orthotropic) plates of various span-to-thickness ratios (a/2h = 5, 10, and 100), showed close agreement, with RZT (G_α) and RZT ($C_{I\alpha}$) producing slightly superior results. For this reason, subsequent discussions concerning homogeneous plates focus exclusively on RZT (G_α) that was originally introduced in [30]. The perturbed transverse-shear approach is assessed by fixing the small scalar at $s = 10^{-5}$ while studying the plate's response by increasing the number of the discretized layers, N.

Results are shown for the maximum values of three response quantities in Table II. These results include the central transverse displacement (deflection), which is averaged across the thickness, $u_z^{\text{ave}}(a/2, a/2)$, the central inplane stress on the top surface, $\sigma_{11}^h(a/2, a/2, h)$, and the edge transverse-shear stress at the midplane, $\tau_{1z}^0(0, a/2, 0)$. The results are normalized with respect to the corresponding solutions of three-dimensional elasticity theory. The response quantities are seen to converge from below as N is increased from 1 to 64. The special case of $N = 1$ corresponds to FSDT ($k^2 = 1$), that is, the zigzag functions are identically zero in this case. For a thin plate (a/2h = 100), the deflection and inplane stress match the exact solution very closely for all values of N, whereas the transverse shear stress converges to the exact solution of three-dimensional elasticity theory as N is increased. For moderately thick (a/2h = 10) and thick (a/2h = 5) plates, all quantities converge to slightly greater values that exceed those of three-dimensional elasticity. The converged results corresponding to RZT (G_α; $N = 64$) were also compared with Reddy's third-order theory and both theories were found to be in close agreement. In both cases, the slightly over estimated results for thick plates may be attributed to the lack of transverse normal flexibility in these theories.

Normalized through-the-thickness distributions for the $\bar{u}_1$, $\bar{\sigma}_{11}$, and $\bar{\tau}_{1z}$ response quantities, corresponding to a thick orthotropic plate (a/2h = 5), are depicted in Figs. 3–5. The special case of $N = 1$ shows a linear variation through the thickness that matches that of FSDT. As N is increased, a nonlinear distribution is achieved [Fig. 3(a)]. A close comparison of the nonlinear, converged solution to the corresponding solutions of three-dimensional elasticity and Reddy's third-order theory is shown in Fig. 3(b). For this thick orthotropic plate, Reddy's theory is perfectly applicable and its predictions are in very close agreement with RZT (G_α; $N = 64$). In

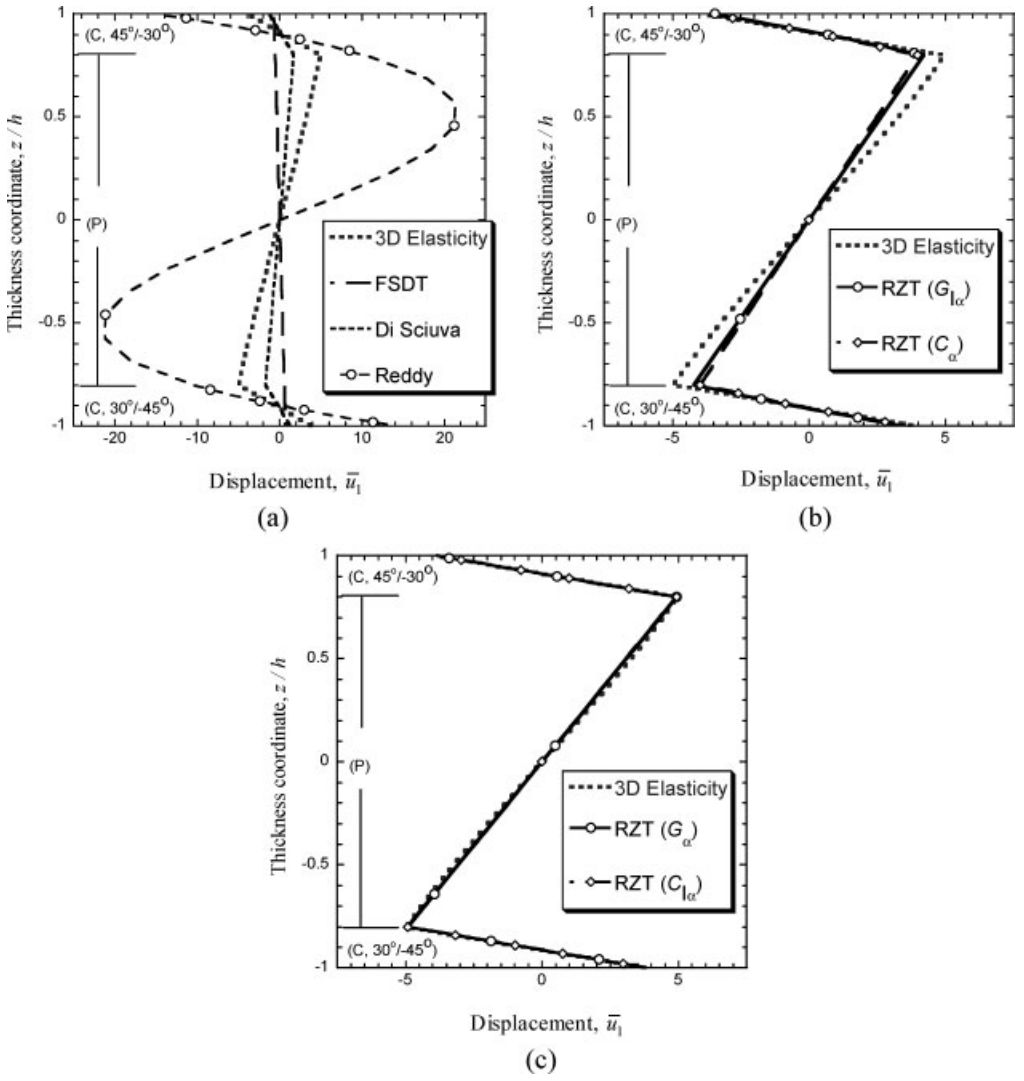

FIG. 6. Through-thickness distribution of inplane displacement for an angle-ply, antisymmetric, sandwich laminate (a/2h = 5).

Figs. 4 and 5, similar comparisons are provided for the inplane stress, $\bar{\sigma}_{11}$, and transverse shear stress, $\bar{\tau}_{1z}$, distributions. Of particular interest is the convergence of transverse shear stress; both RZT (G_α; $N = 64$) and Reddy's parabolic stresses slightly over estimate the maximum value at the midplane; however, RZT (G_α; $N = 64$) is slightly closer to the three-dimensional elasticity solution. An additional study of thinner homogeneous orthotropic plates reveals that all three theories achieve full agreement, demonstrating correct linear distributions for the inplane displacements, and stresses and a parabolic variation of the transverse shear stress through the thickness (not shown).

These results demonstrate that RZT is perfectly suited for predicting accurate parabolic transverse shear stresses, in a piecewise-constant fashion; hence no shear correction factors are required

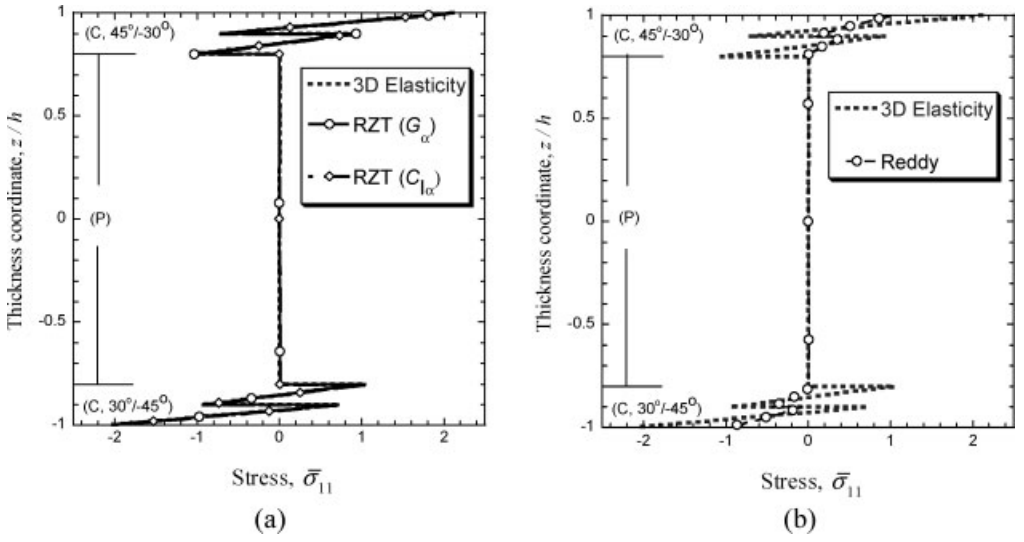

FIG. 7. Through-thickness distribution of inplane stress for an angle-ply, antisymmetric, sandwich laminate (a/2h = 5).

to model homogenous plates. Moreover, for thick plates, accurate nonlinear inplane displacements and stresses consistent with three-dimensional elasticity are obtained in a piecewise-linear fashion. Recall that, similarly, no shear correction factors are needed for heterogeneous composite and sandwich laminates, as discussed in [30].

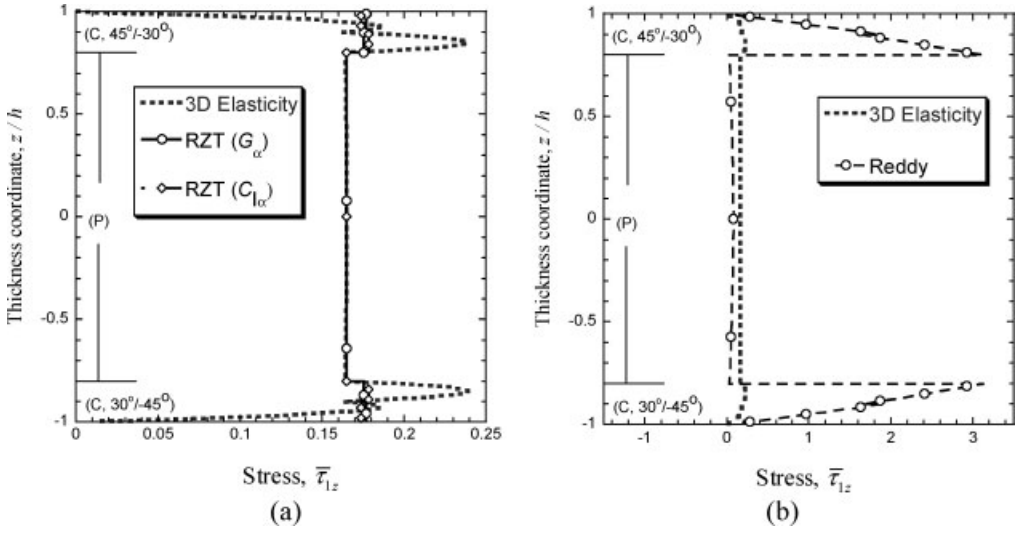

FIG. 8. Through-thickness distribution of transverse-shear stress for an angle-ply, antisymmetric, sandwich laminate (a/2h = 5).

TABLE II. Deflection, inplane stress, and transverse shear stress as a function of the number of discretization layers, N, for homogeneous orthotropic plates (a/2h = 5, 10, and 100); results correspond to RZT (G_α; N) and are normalized with respect to three-dimensional elasticity solutions.

	a/2h = 5			a/2h = 10			a/2h = 100		
N	u_z^{ave}	σ_{11}^h	τ_{1z}^0	u_z^{ave}	σ_{11}^h	τ_{1z}^0	u_z^{ave}	σ_{11}^h	τ_{1z}^0
1	0.948	0.870	0.591	0.976	0.964	0.565	1.000	1.000	0.556
4	1.002	0.972	0.946	0.999	0.993	0.925	1.000	1.000	0.917
16	1.024	1.015	1.025	1.009	1.005	1.003	1.000	1.000	0.995
64	1.026	1.017	1.030	1.009	1.006	1.008	1.000	1.000	1.000

B. Assessment of Four Zigzag-Function Methods for Heterogeneous Laminates

This section focuses on the assessment of the four variants of RZT presented in Section IV. The selected laminate has a high degree of material heterogeneity and anisotropy and is the most challenging of the many laminates examined in [30]. The laminate is an angle-ply, antisymmetric, thick sandwich plate with the aspect ratio $a/2h = 5$. The five-layer sandwich has two stiff carbon-epoxy face sheets and a thick and very compliant PVC core. The normalized lamina-thickness distribution, $h^{(k)}/h$, starting from the first layer, is given by (0.05/0.05/0.8/0.05/0.05); the corresponding lamina orientation angles are $(30^\circ/-45^\circ/0^\circ/45^\circ/-30^\circ)$; the material distribution is given by (C/C/P/C/C), where the labels C and P correspond to the carbon-epoxy and PVC materials, respectively. The PVC material is modeled as an isotropic material with Young's modulus $E = 1.040 \times 10^{-1}$ GPa and Poisson ratio $v = 0.3$. The mechanical properties of the carbon-epoxy plies (material C) are the same as those reported in Section 5.1.

Comparisons of results for the center deflection, which is normalized with respect to the three-dimensional elasticity solution, are presented in Table III. The results are obtained from FSDT, Reddy's third-order theory, Di Sciuva's zigzag theory, and the four variants of RZT. The results demonstrate that RZT (G_α) and RZT ($C_{I\alpha}$) underestimate the deflection by less than 0.1%, compared to 12% by RZT ($G_{I\alpha}$) and RZT (C_α). By comparison, FSDT underestimates the deflection by about 92%, and Reddy and Di Sciuva theories underestimate the deflection by about 62% and 10%, respectively. Note that Di Sciuva's solution is only approximate, due to the presence of angle plies in this laminate (refer to [30] for further details). Also, FSDT's deflection is expected to improve by employing lamination-appropriate shear correction factors.

Figures 6–8 demonstrate through-the-thickness distributions for the $\bar{u}_1$, $\bar{\sigma}_{11}$, and $\bar{\tau}_{1z}$ quantities for the sandwich laminate where, for comparison, three-dimensional elasticity and Reddy theories are used. Figure 6 shows that RZT (G_α) and RZT ($C_{I\alpha}$) yield superior $\bar{u}_1$ displacement predictions and, as expected, FSDT and Reddy theories are the least accurate. Figures 7 and 8 depict the inplane stress, $\bar{\sigma}_{11}$, and transverse shear stress, $\bar{\tau}_{1z}$, distributions, respectively, where the comparisons are narrowed to the best performing zigzag theories, RZT (G_α) and RZT ($C_{I\alpha}$), and Reddy's third-order theory.

TABLE III. Center deflection normalized with respect to three-dimensional elasticity solution for angle-ply, sandwich laminate ($a/2h = 5$).

Normalized center deflection, $w_{\text{Center(Theory)}}/w_{\text{Center(3D Elasticity)}}$						
FSDT	Reddy	RZT (C_α)	RZT ($G_{I\alpha}$)	Di Sciuva	RZT (G_α)	RZT ($C_{I\alpha}$)
0.075	0.382	0.879	0.882	0.902	0.999	0.999

For both stress components, RZT (G_α) and RZT ($C_{I\alpha}$) produce highly accurate results. By comparison, Reddy's theory underestimates the maximum inplane stress by about 50% [Fig. 7(b)], and over estimates the maximum transverse shear stress by a factor of 20 [Fig. 8(b)]; this latter result is typical for a higher-order theory applied to a sandwich analysis. Furthermore, a close examination of the transverse shear stress in the face sheets [Fig. 8(a)] indicates that although both the RZT (G_α) and RZT ($C_{I\alpha}$) predictions are nearly equally accurate, RZT ($C_{I\alpha}$) solutions in the face sheets are slightly superior. Integration of three-dimensional elasticity equilibrium equations, while invoking RZT's inplane stresses, produces highly accurate, continuous through-the-thickness, transverse shear stresses (not shown; for details refer to [30]).

VI. CONCLUSIONS

The RZT has been reformulated from a multi-scale perspective and produced superior results over a wide range of material systems and plate aspect ratios. Four sets of zigzag functions, derived from the condition of limiting homogeneity of transverse-shear properties, provide viable modeling alternatives; however, only two sets of these functions have demonstrated superior predictions. For all material systems, there are no requirements for shear correction factors to yield accurate results. This variationally consistent theory, derived from the virtual work principle, requires simple C^0-continuous kinematic approximations for developing computationally efficient finite elements.

To model homogeneous plates effectively using the full power of zigzag kinematics, a multilayered modeling approach that employs infinitesimally perturbed transverse-shear stiffness properties has been demonstrated. The methodology permits excellent predictions of all response quantities and does not increase the computational effort since the number of kinematic variables remains unchanged.

Results of analytic solutions have been presented which reveal that RZT is a highly accurate theory over a wide range of span-to-thickness ratios and material systems, including very challenging sandwich plates that exhibit a high degree of transverse-shear flexibility, anisotropy, and heterogeneity. The theory is therefore ideally suited for large-scale finite element analyses and has the potential to be successfully employed in designing high-performance homogeneous, laminated composite, and sandwich aerospace structures.

References

1. E. Reissner, The effect of transverse shear deformation on the bending of elastic plates, ASME J Appl Mech 12 (1945), 69–77.
2. R. D. Mindlin, Influence of rotatory inertia and shear deformation on flexural motions of isotropic elastic plates, ASME J Appl Mech 18 (1951), 31–38.
3. J. M. Whitney and N. J. Pagano, Shear deformation in heterogeneous anisotropic plates, J Appl Mech 37 (1970), 1031–1036.
4. S. B. Dong and F. K. W. Tso, On a laminated orthotropic shell theory including transverse shear deformation, J Appl Mech 39 (1972), 1091–1097.
5. E. Reissner, Reflections on the theory of elastic plates, Appl Mech Rev 38 (1985), 1453–1464.
6. L. Librescu, A. A. Khdeir, and J. N. Reddy, A comprehensive analysis of the state of stress of elastic anisotropic flat plates using refined theories, Acta Mechanica 70 (1987), 57–81.
7. K. Noor and W. S. Burton, Assessment of shear deformable theories for multilayered composite plates, Appl Mech Rev 42 (1989), 1–12.

8. D. Liu and X. Li, An overall view of laminate theories based on displacement hypothesis, J Compos Mater 30 (1996), 1539–1561.
9. J. N. Reddy, A simple higher-order theory for laminated composite plates, J Appl Mech 51 (1984), 745–752.
10. A. Tessler, An improved plate theory of {1,2}-order for thick composite laminates, Int J Solids Struct 30 (1993), 981–1000.
11. G. M. Cook and A. Tessler, A {3,2}-order bending theory for laminated composite and sandwich beams, Composites Part B 29 (1998), 565–576.
12. A. Barut, E. Madenci, T. Anderson, and A. Tessler, Equivalent single layer theory for a complete stress field in sandwich panels under arbitrary distributed loading, Composite Struct 58 (2002), 483–495.
13. J. N. Reddy, A generalization of two-dimensional theories of laminated composite plates, Commun Appl Numer Methods 3 (1987), 173–180.
14. X. Lu and D. Liu, An interlaminar shear stress continuity theory for both thin and thick composite laminates, J Appl Mech 59 (1992), 502–509.
15. H. G. Allen, Analysis and design of structural sandwich panels, Pergamon, Oxford (UK), 1969.
16. Y. Frostig, M. Baruch, O. Vilnay, and I. Sheinman, High-order theory for sandwich-beam behavior with transversely flexible core, J Eng Mech 118 (1992), 1026–1043.
17. S. R. Swanson and J. Kim, Comparison of a higher order theory for sandwich beams with finite element and elasticity analyses, J Sandwich Struct Mater 2 (2000), 33–49.
18. P. P. Camanho, C. G. Dávila, and D. R. Ambur, Numerical simulation of delamination growth in composite materials, NASA/TP-2001-211041, 2001.
19. P. P. Camanho and C. G. Dávila, Mixed-mode decohesion finite elements for the simulation of delamination in composite materials, NASA/TP-2002-211737, 2002.
20. M. Di Sciuva, A refinement of the transverse shear deformation theory for multilayered orthotropic plates, Proceedings of 7th AIDAA National Congress, 1983; also in L'aerotecnica missili e spazio, 1984, pp. 84–92.
21. M. Di Sciuva, Development of an anisotropic, multilayered, shear-deformable rectangular plate element, Comput Struct 21 (1985), 789–796.
22. M. Di Sciuva, Bending, vibration and buckling of simply supported thick multilayered orthotropic plates: an evaluation of a new displacement model, J Sound Vibr 105 (1986), 425–442.
23. M. Di Sciuva, An improved shear-deformation theory for moderately thick multilayered anisotropic shells and plates, ASME J Appl Mech 54 (1987), 589–596.
24. M. Di Sciuva, Multilayered anisotropic plate models with continuous interlaminar stresses, Compos Struct 22 (1992), 149–168.
25. M. Cho and R. R. Parmenter, An efficient higher order plate theory for laminated composites, Compos Struct 20 (1992), 113–123.
26. R. C. Averill, Static and dynamic response of moderately thick laminated beams with damage, Compos Eng 4 (1994), 381–395.
27. A. Tessler, M. Di Sciuva, and M. Gherlone, Refinement of Timoshenko beam theory for composite and sandwich beams using zigzag kinematics, NASA/TP-2007-215086, National Aeronautics and Space Administration, Washington, D. C., 2007.
28. A. Tessler, M. Di Sciuva, and M. Gherlone, Refined zigzag theory for laminated composite and sandwich plates, National Aeronautics and Space Administration, Washington, D. C., 2009.
29. A. Tessler, M. Di Sciuva, and M. Gherlone, A refined zigzag beam theory for composite and sandwich beams, J Compos Mater 43 (2009), 1051–1081.

30. A. Tessler, M. Di Sciuva, and M. Gherlone, A consistent refinement of first-order shear-deformation theory for laminated composite and sandwich plates using improved zigzag kinematics, J Mech Mater Struct 5 (2010), 341–367.

31. M. Di Sciuva, M. Gherlone, and A. Tessler, A robust and consistent first-order zigzag theory for multilayered beams, R. Gilat and L. Banks-Sills, editors, Advances in Mathematical Modelling and Experimental Methods for Materials and Structures: The Jacob Aboudi Volume, Springer, New York, 2009.

32. D. Guzzafame, Finite element formulation for the analysis of multilayered plates in cylindrical bending, M.S. Thesis, Politecnico di Torino, 2006.

33. C. Fasano, Development and implementation of interface techniques for beam finite elements (in Italian), M.S. Thesis, Politecnico di Torino, 2008.

34. M. Gherlone, A. Tessler, and M. Di Sciuva, A C^0-continuous two-node beam element based on refined zigzag theory and interdependent interpolation, MAFELAP 2009 Conference, Brunel University, London (UK), 2009.

35. D. Versino, M. Mattone, M. Gherlone, A. Tessler, and M. Di Sciuva, An efficient, C^0-continuous triangular element for laminated composite and sandwich plates with improved zigzag kinematics, MAFELAP 2009 Conference, Brunel University, London (UK), 2009.

36. N. J. Pagano, Exact solutions for composite laminates in cylindrical bending, J Compos Mater 3 (1969), 398–411.

37. A. K. Noor and W. S. Burton, Three-dimensional solutions for antisymmetrically laminated anisotropic plates, Trans ASME 57 (1990), 182–188.